Major and trace element distributions in manganese nodules and micronodules as well as abyssal clay from the Clarion-Clipperton abyssal plain, Northeast Pacific

O.G. Duliu, V. Alexe, Jacques Moutte, S.A. Szobotca

Geo-Marine Letters, 2009, 29(2), 71-83, doi : 10.1007/s00367-008-0123-5.

Major and trace element distributions in manganese nodules and micronodules as well as abyssal clay from the Clarion-Clipperton abyssal plain, Northeast Pacific

O.G. DULIU[(1)]*, V. ALEXE[(2)], JACQUES MOUTTE[(3)], S.A. SZOBOTCA[(4)]

[(1)] *Department of Atomic & Nuclear Physics, University of Bucharest, P.O. Box MG-11, 077125 Magurele, (Ilfov), Romania*
[(2)] *Geological Institute of Romania, 1 Caransebes Street, 012271 Bucharest, Romania*
[(3)] *Ecole Nationale Supérieure des Mines de Saint Etienne, Centre SPIN ; Département GENERIC, 158 Cours Fauriel ; 42023 Saint-Étienne Cedex 2, France*
[(4)] *National Institute for Marine Geology and Geoecology, 23-25 Dimitrie Onciu Street, 024053 Bucharest, Romania*

Abstract

The contents of seven major components (TiO_2, Fe_2O_3, MgO, CaO, Na_2O, K_2O and P_2O_5) and 15 trace elements (Sc, V, Cr, Ni, Cu, Sr, Y, Zr, Ba, La, Ce, Nd, Eu, Yb and Th) were determined by ICP-AE spectrometry in 27 samples of manganese nodules, micronodules as well as abyssal clay collected by dredging from an area of nearly 1,9802 nautical miles in the central Clarion-Clipperton abyssal plain at a depth of about 4,500 m. Statistical analyses were used to compare among individual as well as pooled datasets, in addition to different indicators such as La/Th, Ni/Cu and LREE/HREE ratios for the Clarion-Clipperton samples, as well as between these and corresponding values for the upper continental crust (UCC), North America Shale Composite (NASC), and igneous Indian and Pacific Mid-Ocean Ridge Basalts (MORBs). The results show significant correlations between major components in the Clarion-Clipperton samples and Pacific Ocean MORB, whereas trace elements (excepting Ni and Cu) correlate better with the UCC and NASC. There is also depletion in LREEs, together with a Ce negative anomaly for all Clarion-Clipperton samples. The nodule, micronodule and abyssal clay datasets each reveal typical clusters of components such as P_2O_5 and Y, La, Nd, Eu, Tb, or Ni and Cu. Compared to abyssal clay, the nodule as well as micronodules show significant enrichment in Ni and Cu; nevertheless, an essentially constant Ni/Cu ratio indicates that all samples come from the sediment surface. The distributions of major components as well as trace elements for the Clarion-Clipperton samples present, to different degrees, characteristics common to both the upper continental crust and Mid-Ocean Ridge Basalt, strongly implying a hydrothermal origin, most probably from East Pacific Rise material transported by the Pacific North Equatorial Current.

I. Introduction

Manganese nodules represent one of the most significant authigenic sediment components in ocean basins. Discovered well over 100 years ago by Murray and Renard (1891) in both the South and North Pacific Ocean, these nodules usually occur in areas of slow sedimentation (about 1–3 mm/103 years) far offshore, where their formation and, therefore, accumulation extend over long periods of time (cf. growth rates are 1–16 mm/106 years; Lalou and Brichet

* Auteur à qui la correspondance devait être adressée : duliu@b.astral.ro

1972, and Bollhöfer *et al.* 1996 respectively). They have been reported in the North and South Pacific Ocean, the North and South Atlantic, as well as the Indian Ocean (Cronan 1977), commonly at the sediment surface but also buried in sediments up to few meters deep and more (Cronan 1977; Jeong *et al.* 1996), in various settings including oceanic plateaus and seamounts, active mid-ocean and inactive ridges, marginal topographic elevations and continental borderland, and deep-sea basins. Their formation results from the weathering of volcanic rocks, precipitation from seawater and hydrothermal solutions, as well as sedimentary diagenetic processes.

Such diversity of location and formation is reflected both in the external appearance and in the chemical composition of manganese nodules. During the 1970s, these formations were extensively investigated as a potential source of nonferrous metals but, with the discovery of new ore resources these past decades, interest in the economic exploitation of manganese nodules has diminished. Nevertheless, together with manganese crusts, they still attract attention as a rich source of information on the physicochemical characteristics of the marine environment in which they have formed (Raab and Meylan 1977; Stoffers *et al.* 1981; Jeong *et al.* 1996), including past climatic changes (*e.g.* Bollhöfer *et al.* 1996; Han *et al.* 2003; Glasby *et al.* 2007).

In studying the complex interrelationships between the nodules and the sediments in which they are generated, it is meaningful to include the characterization of micronodules, as these coexist with abyssal clay and nodules, and between all there occurs a continuous exchange of material. Evidently, a comparative investigation of the distributions of major as well as trace elements in these three constituents of oceanic sediments is of real interest. Furthermore, the difference in size between nodules and micronodules—the latter seldom exceeding 1 mm in diameter, the former seldom smaller than 10 mm—pleads for two different classes of sedimentary formations (Addy 1978, 1979), possibly reflected in their chemical composition.

In identifying similarities and dissimilarities in major and trace element compositions, statistical techniques such as correlation analysis (*cf.* Davis 2002), ternary diagrams such as Sc–La–Th (Taylor and McLennan 1985), or derived indicators such as Ni/Cu (Stoffers *et al.* 1981) and La/Th (Taylor and McLennan 1985) have proven very useful. Rare earth elements (REEs) can furnish additional data concerning the source of material, based on indicators such as the ratio between light REEs (LREEs) and heavy REEs (HREEs), the presence of Ce anomalies, or the existence of a positive correlation between trivalent REEs and P_2O_5, resulting from the role played by phosphoric oxides in REE accumulation (Goldberg 1963; Dubinin and Saval'nov 2000, 2003). Notably, a negative Ce anomaly, together with LREE depletion relative to HREEs are characteristic for hydrothermal iron hydroxides (Murphy and Dymond 1984; Dubinin and Volkov 1986; Dubinin and Saval'nov 2000), whereas a positive Ce anomaly and an enrichment in LREEs are typical for hydrogenic pelagic nodules (Piper 1974; Toth 1980; Hein *et al.* 1988; De Carlo 1991; Dubinin and Saval'nov 2003).

The Clarion-Clipperton Province is among the regions most highly enriched in manganese nodules worldwide, located in the north-eastern equatorial Pacific Ocean, between the Clipperton (south) and Clarion (north) fractures (Figure 1). Here, siliceous pelagic sediments of high porosity may be at the origin of marked diagenetic processes at the sediment-water interface, associated with a high abundance of nodules (Horn *et al.* 1973). In interpreting this interplay, however, it is important to account for the chemical composition of possible source materials, such as terrigenous dust, young volcanic rocks, or hydrothermal vents, most associated with the East Pacific Rise. These can be modelled in terms of the upper continental crust (UCC; Taylor and McLennan 1985), the North America Shale Composite (NASC; Gromet *et al.* 1984), and the Mid-Ocean Ridge Basalt (MORB; Klein and Langmuir 2001).

Within the context presented above, we investigated the occurrence of seven major components (TiO_2, Fe_2O_3, MgO, CaO, Na_2O, K_2O and P_2O_5) and 15 trace elements (Sc, V, Cr, Ni, Cu, Sr, Y, Zr, Ba, La, Ce, Nd, Eu, Yb and Th) in nodules, micronodules and abyssal clay all collected from the same area (about 66 × 30 nautical miles) in the centre of the Clarion-Clipperton Province (Figure 1). Our aim was to provide new evidence of any relationships

between their chemical compositions, ultimately serving to increase our knowledge on the nature and provenance of these deep-sea sediments, with special reference to manganese nodules and micronodules.

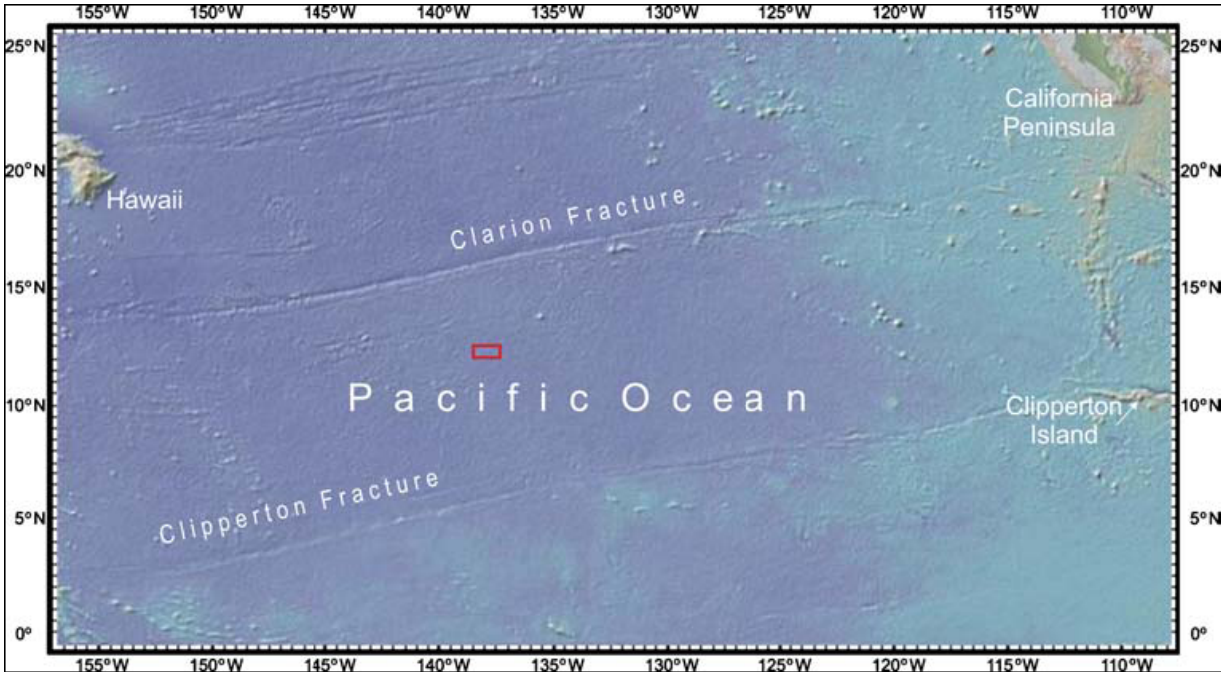

Figure 1: Map showing the location of the Clarion-Clipperton Province, Northeast Pacific, and of the present study site (rectangle; after Marine Geoscience Data System, http://www.marine-geo.org/services/google/create_merc_map.php)

II. Materials and methods

II.1. Samples

Samples of nodules, micronodules and abyssal clay were collected during the 1984 cruise of the Soviet research vessel Akademik Alexandr Karpinski in the Clarion-Clipperton Province of the North Pacific (12–12°40′N and 137°40′–138°50′W; Figure 1), by dredging the seafloor at a depth of about 4,500 m. Onboard ship, a number of nodules were handpicked from the dredged material. Micronodules (0.5–1.0 mm size range) and abyssal clay (<0.65 µm fraction) were separated by wet-sieving. In all, 27 samples were investigated for elemental composition, *i.e.* ten samples from a selected nodule, eight samples of micronodules, and nine of abyssal clay.

Preliminary mineralogical analyses of abyssal clay in the study area, performed by means of X-ray diffraction, showed that illite and smectite account, in various proportions, for about 90% of argillaceous minerals, the remainder being kaolinite and chlorite. The high amount of smectite suggests the presence of an initial pyroclastic material converted into smectite by halmirolysis. Although smectite can have a detrital origin, its enrichment pleads for an authigenic origin (Szobotca 1998). Small amounts of non-argillaceous minerals such as quartz (detrital and possibly aeolian), albite (possibly authigenic) and rarely barite (possibly authigenic) were identified, too.

For our investigations, we chose a typical discoidal manganese nodule, in this case measuring roughly 55.0 by 29.0 mm. It had a smooth upper surface, presumably that most recently exposed to seawater, and a rougher lower surface. Thus, this difference in texture possibly reflects its orientation in the sediment (*cf.* Raab and Meylan 1977; Figure 2). The nodule was cut vertically, revealing an internal structure consisting of a fragment of an older nodule enveloped in younger material. Using a drill with a diameter of 2 mm, we collected ten subsamples, five from the envelope and five from the nucleus (Figure 2). These nodule

samples, as well as the micronodule and abyssal clay samples were manually ground to fine powder by means of an agate mortar.

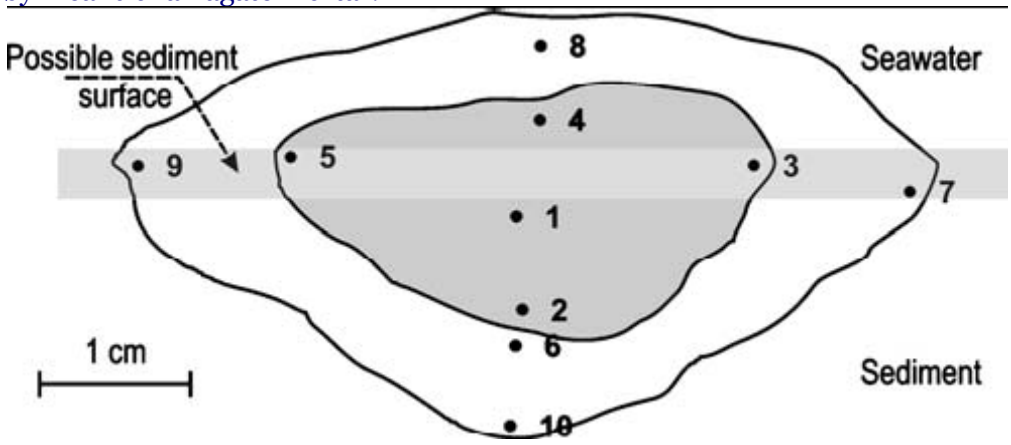

Figure 2: Schematic vertical section through the investigated nodule, showing the positions of the ten sampling points in the envelope and the nucleus (shaded). The inferred sediment surface (cf. main text for further explanation) would correspond to the horizontal nodule axis

II.2. Spectroscopic measurements

About 250 mg of each finely ground sample was poured into a 30 ml PTFE vessel (Savillex), 1 ml 10M HNO_3 and 3 ml 10M HCl added, and the open vessel put into an aluminium block on a hotplate at 120°C and heated until incipient dryness. Then, 3 ml 29 HF was added, and the vessel closed tight and heated at 160°C for 3 days. The vessel was cooled, opened, heated at 110°C until dryness, 3 ml 10M HNO_3 added, followed by heating until dryness, the addition of 3 ml 10M HCl, and heating at 110°C until dryness. This procedure was repeated several times to ensure the elimination of HF without using perchloric acid. Finally, 25 ml 2M HCl was added, the vessel closed and heated a few hours at 90°C to ensure complete dissolution of the salts, and weighed. An MS Excel™ spreadsheet program was used to calculate the dilution ratio.

It is worth mentioning that the classical procedure of acid digestion is to use perchloric acid in conjunction with HF, because the high boiling point of $HClO_4$ makes it most efficient for ensuring a complete elimination of excess HF. However, as $HClO_4$ could not be used in the present case, due to safety regulations, it was replaced by repeated heating–drying steps, first with HNO_3, then with HCl. HNO_3 was used first because it is more efficient than HCl for the elimination of HF and for dissolving fluorides, producing nitrates which are easily dissolved with HCl (Roelandts 1990).

Major elements were determined for each sample directly in the vessel, using a Jobin-Yvone JY 138 Ultratrace ICP-AES sequential high-resolution spectrometer (1 m focal length), for which special software to optimize the drift control has been developed.

Trace elements (including REEs) were determined after these initial ICP analyses. Each vessel was weighed, and then the sample dried at 110°C and diluted with 5 ml 2M HCl. An ion exchange column (Econo-Pac, Bio-Rad Laboratories, Hercules, CA) was charged with 5 g wet resin (Dowex AG50W-X8, 200–400 mesh, Bio-Rad Laboratories) settled to a height of about 60 mm in 2M HCl. After equilibration with 15 ml 2M HCl, the sample was loaded and major elements were washed away with 30 ml 2M HCl, followed by 15 ml 1M HNO_3. REEs were then eluted with 40 ml 5.5 HNO_3, taken to dryness in the same vessel, and diluted with 5 ml 2M HCl. After ICP analysis of this solution, the efficiency of separation was checked by duplicate determinations of Y and Ba before and after separation (*cf.* these elements accompany the REEs, and are more reliably measured). In this way, it was possible to determine with minimum errors the content of only five REEs, i.e. La, Ce, Nd, Eu and Yb.

A relative precision better than 3% was achieved for the spectroscopic measurements, by using a control solution measured after every ten samples, in order to monitor the drift of the

excitation source, which is known as the main source of error in ICP-AES. It should be noted that the MnO contents of all nodule and micronodule samples were systematically higher then 25%, which exceeded the instrument's possibility of correct determination.

II.3. Statistical assessments

Data were pooled to generate an average content of major or of trace elements for each subsystem, *i.e.* the nodule (*i.e.* envelope and nucleus), micronodules and abyssal clay. Comparisons among the Clarion-Clipperton data and corresponding values extracted from the literature for the UCC, NASC, and Pacific and Indian MORBs reference materials are based on correlation analyses (correlation coefficient, r), using the StatSoft™ Statistica 6.0™ program. Significant correlations are set at $p < 0.05$ (cf. the commonly accepted smallest level of significance at which the existence of correlation can be rejected; Davis 2002).

Similarly, interrelationships between individual elements (major as well as trace) for the Clarion-Clipperton samples were investigated. In addition to reporting the complete dataset in a table, we have illustrated the most representative correlations in graphic form.

In some cases (P_2O_5, Sc, Ni and Cu, Th, the four REEs excepting Ce), data for the non-pooled envelope/nucleus, micronodules and abyssal clay, together with those for the abovementioned reference materials were examined further by means of a ternary diagram and a plot of La/Th ratios. The same procedure was chosen also for the REEs, based on a chondrite-normalized diagram.

III. Results

Individual measurements of both major and trace element contents, together with average values and standard deviations for the Clarion-Clipperton nodule, micronodules and abyssal clay are shown in the Table 1, as are the corresponding values for the UCC, NASC and Pacific and Indian MORBs. Note that the P_2O_5 and Y contents are not available for the UCC, so that it was not possible to calculate the corresponding Clarion-Clipperton to UCC ratios in this case. Furthermore, we noted a marked increase in the levels of Cr, Ni and Cu in the equatorial plane of the nodule, corresponding to the sediment-seawater interface for both the envelope and nucleus (Table 1). This aspect was not investigated further in the present study but evidently deserves more attention in future work.

Figure 3 shows the ratios between the contents of each component for the Clarion-Clipperton samples and the UCC (plot I) as well as the Pacific MORB (plot II), the ratios between the contents for the Clarion-Clipperton nodule+micronodules and abyssal clay (plot III), and the ratios between the Pacific+Indian MORBs and the UCC (plot IV). The contents of each of the major components TiO_2, Fe_2O_3, MgO, CaO, Na_2O and K_2O for the Clarion-Clipperton nodule, micronodules and abyssal clay are generally close to the upper continental crust values (cCC/cUCC ratios of 0.40–2.50; Table 1 and Figure 3, plot I). By contrast, the corresponding ratios between the Clarion-Clipperton and the Pacific MORB values are consistently lower than 1 (cCC/cMORB-P ratios of 0.22–0.65), except for K_2O: its levels are up to an order of magnitude higher in the Clarion-Clipperton samples (cCC/cMORB-P ratios for K_2O vary from 5.96 for the nodule nucleus to 14.95 for abyssal clay; Table 1 and Figure 3, plot II). For these major components, the MORB/UCC ratios are similar for the Pacific and Indian oceans—cMORB-P/cUCC ratios vary between 0.70 and 3.50, and cMORB-I/cUCC between 0.80 and 3.70—except for K_2O, which shows much lower ratios of 0.05 and 0.04 for the Pacific and Indian Ocean MORBs respectively (Table 1 and Figure 3, plot IV).

Similarly, the contents of the 11 trace components Sc, V, Cr, Sr, Zr, Ba, La, Ce, Nd, Yb and Th for the Clarion-Clipperton nodule, micronodules and abyssal clay generally do not differ strongly from the upper continental crust values (cCC/cUCC ratios of 0.80 to <19.40). By contrast, the Eu micronodule ratio is relatively high (cCC/cUCC ratio of 29.30; Table 1 and Figure 3). Furthermore, the contents of Ni and Cu are considerably higher in the nodule and micronodules than in the crust (cCC/cUCC ratios of 449.20 and 513.90, and 204.40 and

231.20 respectively; Table 1 and Figure 3, plot I), the trend being less marked for abyssal clay (Ni and Cu cCC/cUCC ratios of 49.30 and 30.70 respectively).

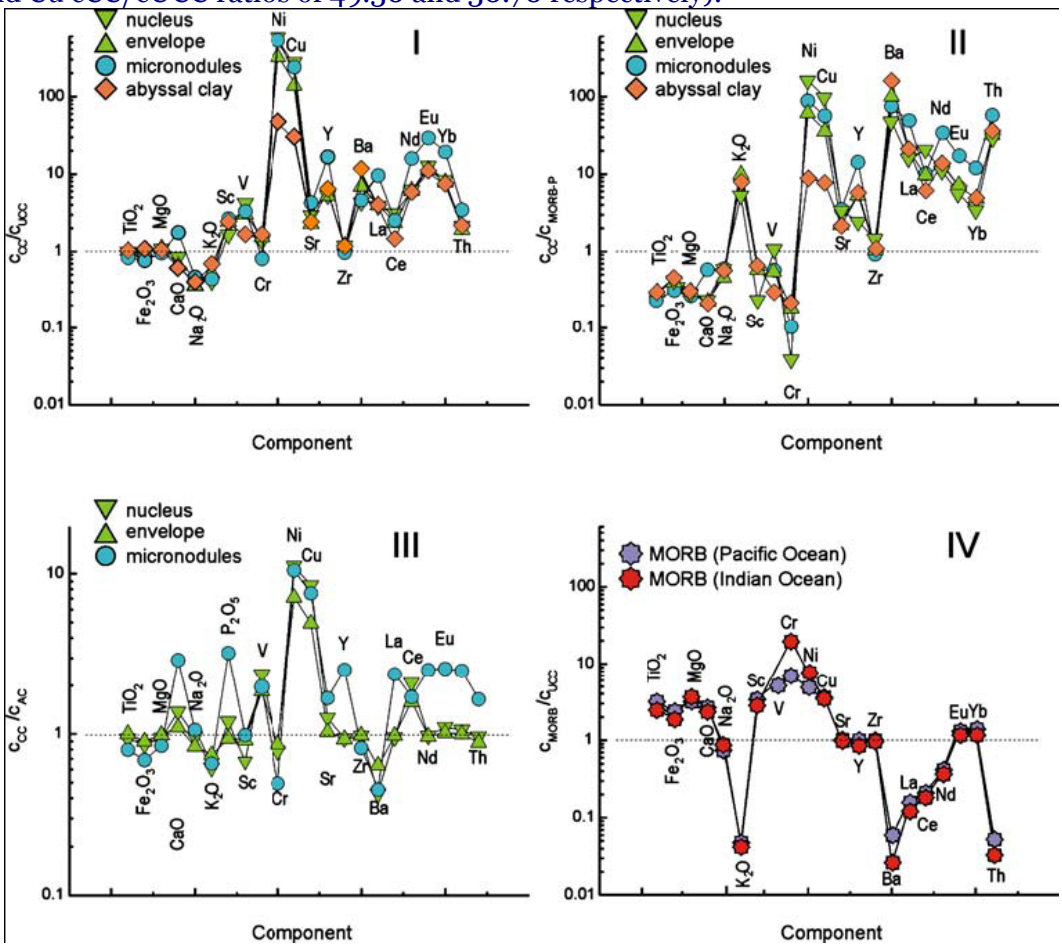

Figure 3: Contents of major and trace elements in the Clarion-Clipperton nodule (envelope and nucleus values shown in green), micronodules (blue) and abyssal clay (orange) normalized to the UCC (plot I) and to Pacific Ocean MORB (plot II), contents for the Clarion-Clipperton nodule and micronodules normalized to the corresponding values for abyssal clay (plot III), as well as contents for the Pacific and Indian Ocean MORBs (purple and red respectively) normalized to the UCC (plot IV; UCC data extracted from Taylor and McLennan 1985; MORBs data extracted from Klein and Langmuir 2001

Compared to the Pacific MORB, for the Clarion-Clipperton samples we found a slight depletion in the trace components Sc and Cr (for Sc, the cCC/cMORB-P ratios are 0.80–0.20 but they are consistently smaller than 0.23 for Cr). By contrast, for Sr, Zr, Ba, La, Ce, Nd, Eu, Yb and Th we recorded enrichments which attained a maximum for Ba (cCC/cMORB-P varies between 89.30 for the nodule and 196 for abyssal clay) and Th (from 39.92 for the nodule to 69.93 for micronodules). Similar enrichments occurred for Ni (cCC/cMORB-P varies from 93.91 for the nodule to 107.44 for micronodules) and for Cu (from 59.53 for the nodule to 67.32 for micronodules; Table 1 and Figure 3, plot II).

Compared to the contents of major components and trace elements in abyssal clay, for the nodule and micronodules we found enrichments only for Ni and Cu (cCC/cAC ratios of 9.10 and 10.41, and 6.66 and 7.53 respectively; Table 1 and Figure 3, plot III), consistent with the finding that, relative to the UCC, abyssal clay is also highly enriched in Ni and Cu. It is emphasised that, within experimental error limits, the Ni/Cu ratios are similarly high for the nodule and micronodule samples (1.70 for nodule nucleus, 1.86 for nodule envelope, 1.78 for micronodules) but slightly lower for abyssal clay (1.29), UCC (0.80) and Pacific Ocean MORB (1.11; Table 1).

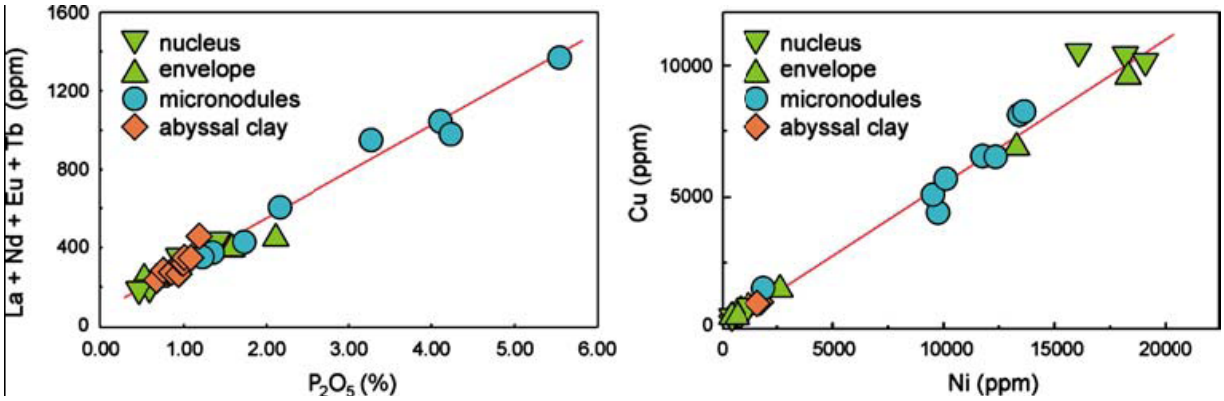

Figure 4: La+Nd+Eu+Tb versus P_2O_5 (left), and Cu versus Ni (right) plots for the Clarion-Clipperton nodule (envelope and nucleus shown in green), micronodules (blue) and abyssal clay (orange)

Statistical analyses indicate significant correlations (p<0.05) between the contents of pooled major elements in the nodule envelope and the nucleus (r=0.9710), the nodule envelope and abyssal clay (r=0.9156), the nodule nucleus and abyssal clay (r=0.9804), and (albeit weaker) the Pacific and Indian Ocean MORBs and the nodule nucleus (r=0.9018 and 0.8505 respectively) as well as micronodules (r=0.8187 and 0.8127 respectively; Table 2).

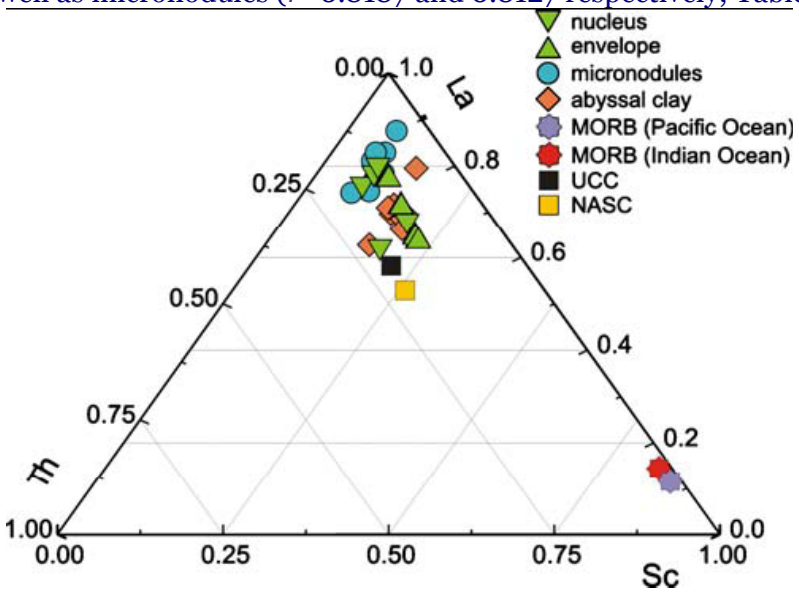

Figure 5: Sc, La and Th ternary diagram for the Clarion-Clipperton nodule (envelope and nucleus shown in green), micronodules (blue) and abyssal clay (orange), and corresponding values for the UCC (black; extracted from Taylor and McLennan 1985), NASC (yellow; extracted from Gromet et al. 1984), as well as the Pacific and Indian Ocean MORBs (purple and red respectively; extracted from Klein and Langmuir 2001)

There is also a significant correlation between the two types of MORB (Pacific and Indian Ocean, r=0.9855).

Analogous analyses of pooled data for all 15 trace components show significant correlations between the nodule nucleus and the envelope (r=0.9633), micronodules and the nodule nucleus and envelope (r=0.9985 and 0.9698 respectively), as well as between abyssal clay and the UCC (r=0.9397; Table 2). Except for a weak but nevertheless significant correlation between Pacific Ocean and Indian Ocean MORBs (r=0.6684), no other significant correlations at p<0.05 were recorded (Table 2).

Statistical analyses performed on only 13 trace elements (cf. Ni and Cu were excluded) show a significant correlation (r>0.9600) between all Clarion-Clipperton samples and the UCC, but the absence of any significant correlation with Pacific and Indian Ocean MORBs (Table 2).

Repeated for all 22 elements and for each subsample type, correlation analyses reveal clusters common for all Clarion-Clipperton samples, such as P2O3, Y, La, Nd, Eu and Tb, Ni and Cu, whereas Sr correlates positively with CaO only in the nodule and micronodules (Table 3, Figure 4). Other observed correlations are restricted to one subsample type and are not discussed further.

A Sc-La-Th ternary diagram (Figure 5) shows the presence of two main clusters for the Clarion-Clipperton samples, which group closer to the UCC and NASC values than to the Pacific and Indian Ocean MORBs. This can largely be explained by a significantly higher content of Th in the Clarion-Clipperton samples than in the MORBs (Table 1).

A La versus Th plot (Figure 6) shows the Clarion-Clipperton values being closely grouped for the nodule (*cf.* data for both the envelope and nucleus indicated) and the abyssal clay samples, but scattering widely for the micronodule samples. The La/Th ratios all exceed 1, indicating enrichment in La relative to Th, particularly for the micronodules. This enrichment has been recorded also for the UCC and NASC, and particularly for the Pacific and Indian Ocean MORBs (Figure 5). Indeed, in the combined dataset, the Clarion-Clipperton micronodules and the MORBs all have La/Th ratios exceeding 6.50; the UCC and particularly the NASC have the lowest ratios of all (less than 3), whereas both the Clarion-Clipperton nodule and abyssal clay have an intermediary value of around 5. Thus, there is a strong difference in La/Th between the Clarion-Clipperton micronodules (7.04±2.61) and the UCC (2.80) and NASC (2.50), the differences being less marked *vis-à-vis* the MORBs.

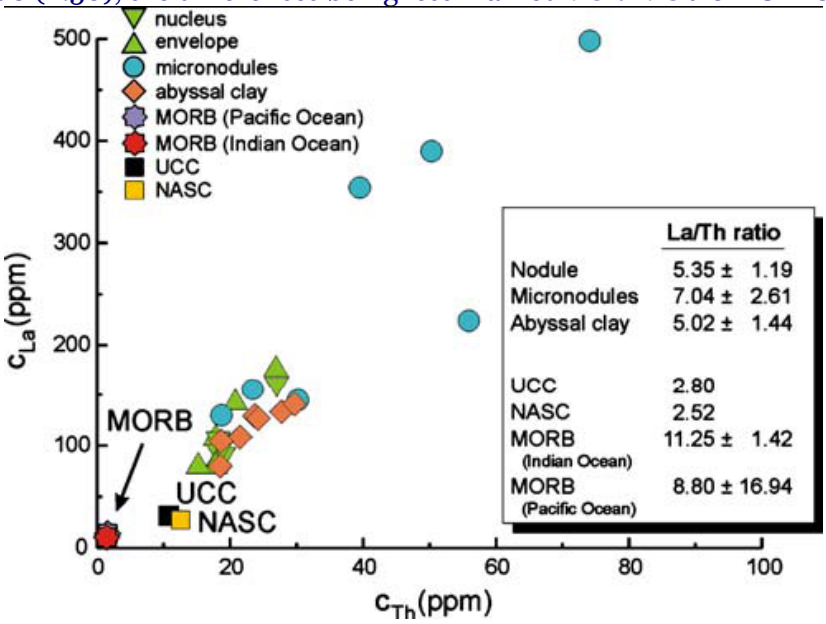

Figure 6: La versus Th contents for the Clarion-Clipperton nodule (envelope and nucleus shown in green), micronodules (blue) and abyssal clay (orange), and corresponding values for the UCC (black; extracted from Taylor and McLennan 1985), NASC (yellow; extracted from Gromet et al. 1984), as well as the Pacific and Indian Ocean MORBs (purple and red respectively; extracted from Klein and Langmuir 2001)

The three chondrite-normalized diagrams in Figure 7 show the contents of the five REEs La, Ce, Nd, Eu and Yb (*cf.* those with contents determined with less than 3% inaccuracy by ICP-AE spectrometry) in the nodule, micronodules and abyssal clay, together with the corresponding data for the UCC, and the Pacific and Indian Ocean MORBs. Compared to the UCC, the contents of La, Nd, Eu and Yb are consistently higher in the Clarion-Clipperton samples, with factors varying between 2.26 for Yb in micronodules and 29.33 for Eu in micronodules. Ce presents a negative anomaly in all three subsystems. Furthermore, the chondrite-normalized contents of La, Nd, Eu and Yb all generally decrease towards the heavy REEs, as do the UCC values, but quite different from both MORBs which have quasi-constant

values for all the REEs. Moreover, the Clarion-Clipperton LREE to HREE ratios (17.60±6.90 for the nodule, 14.50±1.50 for micronodules and 12.90±1.50 for abyssal clay) are substantially larger than the Pacific and Indian MORB values (6.10 and 5.70 respectively) but less than half the corresponding values for the UCC (42.70) and NASC (31.60; Table 1).

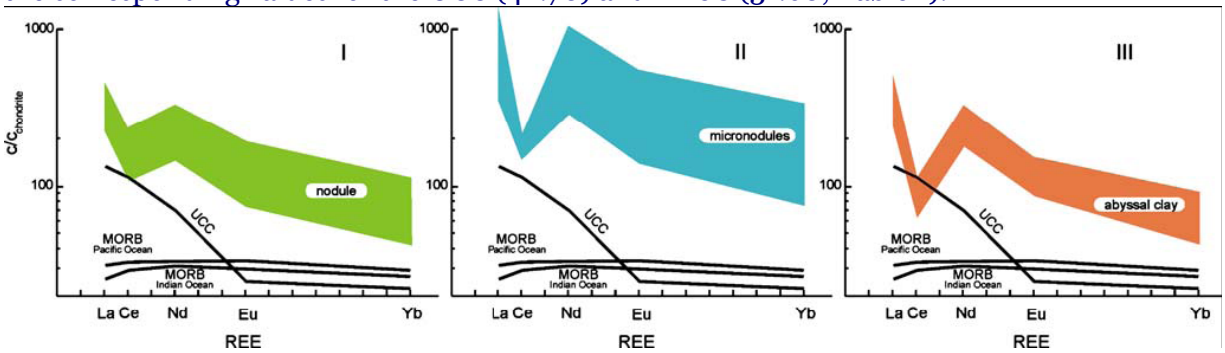

Figure 7: Chondrite-normalized contents of five REEs for the Clarion-Clipperton nodule (plot I, envelope and nucleus shown in green), micronodules (plot II, blue) and abyssal clay (plot III, yellow), and corresponding values for the upper continental crust (UCC, extracted from Taylor and McLennan 1985), as well as the Pacific and Indian Ocean MORBs (extracted from Klein and Langmuir 2001)

IV. Discussion and conclusions

The results show that major components (TiO_2, Fe_2O_3, MgO, CaO, Na_2O, and especially K_2O) of the Clarion-Clipperton nodule, micronodules and abyssal clay all have contents much closer to those recorded for the upper continental crust (and, to a lesser extent, the NASC) than for MORBs. Nevertheless, correlation analyses based on the pooled contents of these major components show a significant relationship between the nodule nucleus and MORBs (Pacific and, to a lesser extent, Indian Ocean MORB), the same being the case for the micronodules but not for abyssal clay. Consistent with the presence of a considerable amount of authigenic smectite in the latter, these apparently contradictory trends can plausibly be explained by a significant igneous source for major components of Clarion-Clipperton nodules and micronodules. Most probably originating from the East Pacific Rise, the igneous material would be transported westwards by the Pacific North Equatorial Current which, by flowing between 10 and 20°N, passes over the study area.

In terms of the pooled contents of these major components, the findings also demonstrate the lack of significant correlation between the micronodules and abyssal clay, and even between the micronodules and the nodule. This can be attributed to the selective enrichment of CaO and P_2O_3 recorded in the micronodule samples, due to the presence of microorganism tests (Stoffers *et al.* 1984; Dekov *et al.* 2003).

In terms of the pooled contents of all 15 trace elements (Sc, V, Cr, Ni, Cu, Sr, Y, Zr, Ba, La, Ce, Nd, Eu, Yb and Th), the finding that significant correlations exist only amongst the nodule nucleus, envelope and micronodules on the one hand and, on the other, between abyssal clay and the UCC can be well explained by the marked enrichment of Ni and Cu recorded for the nodule and micronodules, which would mask any other similarities. Indeed, repeating the analysis without Ni and Cu (13 elements) revealed that all Clarion-Clipperton values are close to the UCC. The lack of any significant relationship with MORB signatures is consistent with the analysis performed by means of a Sc–La–Th ternary diagram which shows the nodule, micronodule and abyssal clay non-pooled data grouped markedly closer to the UCC and NASC values than to the MORBs.

By contrast, a La-Th diagram reveals that all Clarion-Clipperton samples have an average La/Th ratio of 6.16±2.80, a value intermediary between Pacific Ocean MORB (8.80) and UCC (2.80) or NASC (2.52). Moreover, it is emphasised that La and Th contents are markedly higher in the Clarion-Clipperton samples (30–74 ppm for La and 37–202 ppm for Th) than in both MORBs (0.57 ppm for Pacific Ocean and 0.34 ppm for Indian Ocean MORB). This can

largely be explained by the finding that, compared to the MORBs, the Clarion-Clipperton samples are markedly enriched in Th, attributable to the very low solubility of Th in seawater, close to that for REEs and Sc. Consequently, Th tends to accumulate in the sediments (Taylor and McLennan 1985, 1988).

The almost constant Ni to Cu ratios recorded for both the nodule and micronodules in the present study suggest that, during dredging, only nodules and micronodules occurring in the surficial sediment layer were collected. Indeed, as Ni is more mobile than Cu, it generally sharply decreases with sediment depth (Stoffers *et al.* 1984).

The marked Ce negative anomaly recorded in the chondrite-normalized REE diagram for all Clarion-Clipperton samples, i.e. the nodule including its nucleus, the micronodules and abyssal clay, together with the observed relative deficit of LREEs relative to HREEs for these samples plead for a hydrothermal origin of iron oxyhydroxides. This is supported by the finding that REE accumulation in abyssal clay, and transfer from abyssal clay to nodules and micronodules seem to be mediated by phosphates, as indicated by the marked correlation between trivalent REEs and P_2O_5 recorded in the present study (cf. Stoffers and Dubinin 1987; Dubinin and Saval'nov 2003).

Based on preliminary mineralogical analyses of the Clarion-Clipperton abyssal clay, the presence of detrital smectite and illite and, to a lesser extent, kaolinite and chlorite together with small amounts of non-argillaceous minerals suggest a less important transport of terrigenous material from the continent, and a more important contribution of authigenic material, most probable from the East Pacific Rise. This is supported by the observed significant positive correlations between major element contents in Clarion-Clipperton nodules and Pacific Ocean MORB. The lack of good correlation between the major components of Clarion-Clipperton micronodules and abyssal clay argues in favour of a different mechanism of micronodule generation in this region. Furthermore, there is evidence of a local phosphate-mediated enhancement in REEs and possibly other trace elements such as Th which, with time, has shifted their enrichment patterns closer to those of the upper continental crust. Finally, the negative Ce anomaly and depletion in LREEs indicate a hydrothermal origin for Clarion-Clipperton nodules, micronodules and abyssal clay, most probably the East Pacific Rise.

Evidently, the distributions of major and trace elements in nodules, micronodules and abyssal clay on the Clarion-Clipperton abyssal plain present complex signatures reflecting the influence of both the upper continental crust and MORB, as well as probable East Pacific Rise material transport via the Pacific North Equatorial Current.

Acknowledgements

We wish to express our gratitude to two anonymous referees and the journal editors for their valuable suggestions in revising the manuscript.

References

Addy SK (1978) Distribution of Fe, Mn, Cu, Ni and Co in coexisting manganese nodules and micronodules. Mar Geol 28:M9–17

Addy SK (1979) Rare earth elements pattern in manganese nodules and micronodules from South West Atlantic. Geochim Cosmochim Acta 43:1105–1115

Bollhöfer A, Eisenhauer A, Frank N, Pech D, Mangini A (1996) Thorium and uranium isotopes in a manganese nodule from the Peru Basin determined by alpha spectrometry and thermal ionization mass spectrometry (TIMS): are manganese supply and growth related to climate? Geol Rundsch 85:577–585

Cronan DS (1977) Deep-sea nodules, distribution and geochemistry. In: Glasby GP (ed) Marine manganese deposits. Elsevier Oceanographic Series vol 15. Amsterdam, Elsevier, pp 11–46

Davis JC (2002) Statistics and data analysis in geology. Wiley, New York

De Carlo EH (1991) Paleoceanographic implications of rare earth element variability within a Fe-Mn crust from the Central Pacific Ocean. Mar Geol 98:449–467

Dekov VM, Marching V, Rajta I, Uzony I (2003) Fe-Mn micronodules born in metalliferous sediments of two spreading centers, the East Pacific Rise and Mid-Atlantic Ridge. Mar Geol 199:101–121

Dubinin AV, Saval'nov VN (2000) Geochemistry of rare earth elements in micro and macronodules from the Pacific bioproductive zone. Lithol Miner Resources 35:19–31 (translated from Litologiya i Poleznye Iskopaemye no 1, pp 25–39)

Dubinin AV, Saval'nov VN (2003) Geochemistry of the manganese ore process in the ocean: evidence from rare earth elements. Lithol Miner Resources 38:19–31 (translated from Litologiya i Poleznye Iskopaemye no 2, pp 115–125)

Dubinin AV, Volkov II (1986) Rare earth elements in metalliferous sediments of the Eastern Pacific Rise (in Russian). Geokhimiya 5:645–662

Glasby GP, Ren X, Shi X, Pulyaeva IA (2007) Co-rich Mn crusts from the Magellan Seamount cluster: the long journey through time. Geo-Mar Lett 27:315–323 doi:10.1007/s00367-007-0055-5

Goldberg ED (1963) Rare earth elements in the marine environment. J Geophys Res 68:4209–4217

Gromet LP, Haskin LA, Korotev RL, Dymek RF (1984) The "North American shale composite": its compilation, major and trace element characteristics. Geochim Cosmochim Acta 48:2469–2482

Han X, Jin X, Yang S, Fietzke J, Eisenhauer A (2003) Rhythmic growth of Pacific ferromanganese nodules and their Milankovitch climatic origin. Earth Planet Sci Lett 211:143–157

Hein JR, Schwab WC, Davis AS (1988) Cobalt- and platinum-rich ferromanganese crusts and associated substrate rocks from the Marshall Islands. Mar Geol 78:255–283

Horn DR, Delach MN, Horn BM (1973) Metal content of the ferromanganese deposits of the oceans. Tech Rep Off Int Decade Ocean Explor 1:1–78

Jeong KS, Kanf JK, Lee KY, Jung HS, Chi SB, Ahn SJ (1996) Formation and distribution of manganese nodule deposits in the northwest margin of Clarion-Clipperton fracture zones, Northeast Equatorial Pacific. Geo-Mar Lett 16:123–131 doi:10.1007/BF02202607

Klein E, Langmuir C (2001) GERM MORB data by ocean basin, depth, and MORB type. http://earthref.sdsc.edu/GERM/data/klein/MORB_ocean.htm

Lalou C, Brichet E (1972) The signification of radiochemical measurements in evaluating the growth ratio of manganese nodules. C R Acad Sci Paris 275 D:815–818

Murphy K, Dymond J (1984) Rare earth element fluxes and geochemical budget in the Eastern Equatorial Pacific. Nature 307:444–447

Murray J, Renard AF (1891) Deep sea deposits. Report Scientific Results Voyage H.M.S. Challenger. Neil, London. http://www.19thcenturyscience.org/HMSC/HMSC-Reports/1891-DeepSeaDeposits/htm/doc.html

Piper DZ (1974) Rare earth elements in ferromanganese nodules and other marine phases. Geochim Cosmochim Acta 38:1007–1022

Raab WJ, Meylan MA (1977) Morphology. In: Glasby GP (ed) Marine manganese deposits. Elsevier Oceanographic Series vol 15. Amsterdam, Elsevier, pp 109–146

Roelandts I (1990) Inductively coupled plasma determination of nine rare-earth elements in sixty international geochemical reference samples. Geostand Newslett 14:137–147

Stoffers II, Dubinin AV (1987) Rare earth elements in hydrothermal accumulations of iron and manganese in the ocean (in Russian). Litologiya Poleznye Iskopaemye 6:40–56

Stoffers P, Glasby GP, Thijssen T, Shrivatsava PC, Melguen M (1981) The geochemistry of coexisting manganese nodules, micronodules, sediments and pore water from five areas in equatorial and S.W. Pacific. Chem Erde 40:273–293

Stoffers P, Sioulas A, Glasby GP, Schmitz W, Mangini A (1984) Sediments and micronodules in the Northern and Central Peru Basin. Geol Rundsch 73:1055–1080

Szobotca SA (1998) Petrological and geochemical study of abyssal sediments from the Central Pacific Ocean with special emphasis to manganese nodules (in Romanian). PhD Dissertation, University of Bucharest, Bucharest

Taylor SR, McLennan SM (1985) The continental crust, its composition, evolution. Blackwell, Oxford

Taylor SR, McLennan SM (1988) The significance of the rare earth in geochemistry and cosmochemistry. In: Gschneidner KA, Eyring L (eds) Handbook of Physics and Chemistry of Rare Earths, vol 11. Amsterdam, Elsevier, pp 485–578

Toth JR (1980) Deposition of submarine crusts rich in manganese and iron. Geol Soc Am Bull 91:44–54

Geo-Marine Letters, 2009, 29(2), 71-83, doi : 10.1007/s00367-008-0123-5.

Tables

Table 1: Contents (with corresponding average values, aver., and standard deviations, SD) of major components and trace elements in the Clarion-Clipperton nodule (n=10), micronodules (n=8) and abyssal clay (n=9), as well as the corresponding ratios for Clarion-Clipperton (c_{CC}) vs. upper continental crust (c_{UCC}; extracted from Taylor and McLennan 1985) and vs. abyssal clay (c_{AC}; present study)

Sample	TiO_2	Fe_2O_3	MgO	CaO	Na_2O	K_2O	P_2O_5	Sc	V	Cr	Ni	Cu	Sr	Zr	La	Ce	Nd	Eu	Yb	Y	Ba	Th
Nodule nucleus																						
1	0.51	5.27	2.32	2.87	1.80	0.96	0.50	9.62	372.00	9.57	19,036.00	10,141.00	561.00	195.00	90.70	329.00	130.00	8.12	11.50	99.80	1,757.00	19.00
2	0.54	5.49	2.22	2.46	1.20	2.00	0.65	26.10	115.00	56.50	1,137.00	776.00	271.00	148.00	93.70	113.00	123.00	8.23	13.20	182.00	4,190.00	18.30
3	0.43	4.03	2.71	5.51	1.95	1.12	2.09	17.30	322.00	27.10	18,14.00	10,40.00	560.00	119.00	161.00	225.00	230.00	16.90	28.20	364.00	1,63800	27.00
4	0.56	5.53	2.33	2.15	1.31	2.22	0.64	26.20	107.00	66.20	357.00	401.00	262.00	145.00	92.10	113.00	117.00	7.52	12.60	180.00	4,159.00	30.00
5	0.40	3.43	2.16	4.48	1.95	1.06	1.57	15.00	300.00	70.00	16,120.00	10,570.00	524.00	106.00	143.00	195.00	202.00	14.50	25.00	304.00	1,522.00	20.80
Aver.	0.48	4.75	2.35	3.49	1.64	1.47	1.09	18.84	243.20	45.87	10,958.00	6,459.00	435.60	142.60	116.10	195.00	160.40	11.05	18.10	225.96	2,653.20	23.02
SD	0.07	0.96	0.21	1.44	0.36	0.59	0.70	7.23	123.50	26.36	9,385.02	5,362.84	155.12	34.20	33.40	89.87	51.92	4.33	7.87	106.19	1,391.28	5.19
c_{CC}/c_{UCC}	0.97	0.95	1.07	0.83	0.42	0.43		1.71	4.05	1.31	547.90	258.36	2.99	1.17	3.87	3.05	6.17	12.56	8.23	6.15	4.82	2.15
c_{CC}/c_{AC}	0.93	0.85	0.94	1.36	0.95	0.61	1.18	0.67	2.34	0.78	11.10	8.41	1.24	0.96	0.94	2.05	0.97	1.09	1.05	0.93	0.43	0.95
Nodule envelope																						
6	0.56	5.44	2.37	1.97	1.28	2.21	0.57	27.90	108.00	68.70	375.00	424.00	270.00	142.00	82.70	105.00	107.00	7.06	12.40	172.00	4,206.00	17.80
7	0.35	3.44	2.22	3.41	1.86	0.91	0.93	11.90	325.00	18.20	18,282.00	9,577.00	459.00	110.00	108.00	193.00	154.00	10.30	16.00	191.00	1,426.00	17.80
8	0.59	5.95	2.44	1.75	1.53	2.39	0.47	28.80	120.00	78.10	472.00	438.00	257.00	150.00	80.70	110.00	102.00	6.51	10.60	143.00	4,326.00	17.80
9	0.55	4.67	2.99	3.93	1.29	1.43	1.41	26.10	263.00	30.50	13,245.00	6,840.00	470.00	154.00	177.00	210.00	237.00	14.80	25.60	324.00	3,904.00	26.90
10	0.55	5.44	2.32	2.93	1.20	1.92	0.93	33.40	137.00	54.80	2,677.00	1,536.00	349.00	159.00	147.00	139.00	192.00	12.40	20.90	289.00	5,307.00	26.20
Aver.	0.52	4.99	2.47	2.80	1.43	1.77	0.86	25.62	190.60	50.06	7,010.20	3,763.00	361.00	143.00	119.08	151.40	158.40	10.21	17.10	223.80	3,833.80	21.30
SD	0.10	0.98	0.30	0.93	0.27	0.60	0.37	8.13	97.45	25.27	8,238.28	4,196.27	100.90	19.47	41.99	47.92	57.33	3.52	6.17	78.39	1,445.12	4.80
c_{CC}/c_{UCC}	1.04	1.00	1.12	0.67	0.37	0.52		2.33	3.18	1.43	350.51	150.52	2.48	1.18	3.97	2.37	6.09	11.61	7.77	6.09	6.97	1.99
c_{CC}/c_{AC}	1.00	0.89	0.98	1.09	0.83	0.74	0.93	0.91	1.84	0.85	7.10	4.90	1.03	0.97	0.97	1.59	0.96	1.01	0.99	0.92	0.62	0.88
Micronodules																						
11	0.33	3.35	1.91	14.70	1.46	1.02	1.21	13.10	237.00	25.80	12,319.00	6,520.00	883.00	127.00	130.00	161.00	203.00	12.10	18.60	234.00	1,899.00	18.70
12	0.55	3.84	2.21	6.08	1.73	1.75	3.27	34.90	225.00	33.80	9,535.00	5,085.00	619.00	143.00	355.00	203.00	521.00	30.90	52.50	756.00	4,877.00	39.50
13	0.43	3.90	2.25	4.16	1.55	1.65	1.74	20.20	222.00	27.60	11,792.00	6,532.00	475.00	118.00	156.00	137.00	238.00	15.10	25.70	339.00	2,524.00	23.40
14	0.35	3.26	2.11	7.85	1.83	1.39	4.21	35.20	193.00	22.50	9,721.00	4,461.00	595.00	135.00	410.00	166.00	505.00	31.50	48.20	708.00	3,177.00	24.00
15	0.38	3.61	2.04	7.87	1.91	1.49	4.09	31.40	188.00	22.60	10,118.00	5,645.00	565.00	111.00	390.00	164.00	572.00	35.20	55.00	870.00	2,597.00	50.30
16	0.43	4.28	2.24	5.00	2.14	1.52	2.14	22.30	242.00	33.70	13,534.00	8,298.00	516.00	117.00	224.00	168.00	328.00	20.30	35.00	457.00	2,201.00	55.90
17	0.45	4.16	2.40	4.10	1.84	1.68	1.38	19.20	230.00	26.60	13,391.00	8,151.00	467.00	112.00	145.00	149.00	214.00	13.70	23.20	309.00	2,509.00	30.20
18	0.39	4.18	1.70	9.37	2.03	2.01	5.55	43.20	82.50	38.00	1,819.00	1,540.00	538.00	109.00	498.00	142.00	740.00	47.70	82.90	1,194.00	2,580.00	74.10
Aver.	0.41	3.82	2.11	7.39	1.81	1.56	2.95	27.44	202.44	28.83	10,278.63	5,779.00	582.25	121.50	288.50	161.25	415.13	25.81	42.64	608.38	2,795.50	39.51
SD	0.07	0.39	0.22	3.51	0.23	0.29	1.57	10.23	52.23	5.70	3,76436	2,18088	132.77	12.33	141.83	20.45	197.79	12.57	21.39	331.31	916.28	19.28
c_{CC}/c_{UCC}	0.83	0.77	0.96	1.76	0.46	0.46		2.49	3.37	0.82	513.93	231.16	4.00	1.00	9.62	2.52	15.97	29.33	19.38	16.55	5.08	3.69
c_{CC}/c_{AC}	0.79	0.68	0.84	2.89	1.05	0.65	3.19	0.98	1.95	0.49	10.42	7.53	1.66	0.82	2.35	1.70	2.50	2.55	2.47	2.51	0.45	1.63

Geo-Marine Letters, 2009, 29(2), 71-83, doi : 10.1007/s00367-008-0123-5.

Sample	TiO_2	Fe_2O_3	MgO	CaO	Na_2O	K_2O	P_2O_5	Sc	V	Cr	Ni	Cu	Sr	Zr	La	Ce	Nd	Eu	Yb	Y	Ba	Th
Abyssal clay																						
20	0.52	5.31	2.37	2.55	1.35	2.39	0.94	26.50	122.00	76.30	1,674.00	1,040.00	299.00	147.00	125.00	104.00	168.00	10.40	18.00	251.00	4,207.00	23.80
21	0.56	5.59	2.43	2.19	1.29	2.58	0.74	28.40	114.00	71.10	525.00	479.00	276.00	151.00	109.00	91.10	151.00	9.14	15.50	221.00	4,444.00	22.10
22	0.50	5.69	3.12	2.81	1.50	2.54	1.17	33.40	103.00	37.20	1,492.00	967.00	617.00	196.00	183.00	94.90	236.00	13.20	22.70	330.00	11,831.00	14.50
23	0.53	5.27	2.29	2.41	1.25	2.38	0.83	27.00	105.00	63.20	678.00	563.00	281.00	144.00	106.00	89.40	148.00	9.44	16.70	222.00	4,684.00	19.90
24	0.36	5.50	2.93	2.55	4.50	1.80	0.92	28.10	70.30	27.90	423.00	519.00	507.00	169.00	111.00	60.70	133.00	7.41	10.50	160.00	12,997.00	38.40
25	0.57	5.77	2.37	2.73	1.28	2.52	0.97	27.80	112.00	66.40	1,165.00	888.00	287.00	137.00	123.00	109.00	169.00	10.90	19.50	265.00	4,125.00	24.20
26	0.52	5.26	2.30	2.85	1.28	2.28	1.01	26.40	107.00	59.30	1,755.00	1,203.00	290.00	119.00	128.00	106.00	184.00	11.40	19.90	277.00	3,884.00	26.90
27	0.53	5.45	2.32	2.22	1.58	2.34	0.65	25.10	95.40	62.00	840.00	702.00	283.00	122.00	87.20	90.80	124.00	7.48	12.90	175.00	4,334.00	19.80
28	0.63	6.41	2.47	2.74	1.48	2.83	1.07	29.90	106.00	66.20	330.00	549.00	317.00	148.00	134.00	109.00	179.00	11.80	19.70	283.00	4,888.00	28.40
Aver.	0.52	5.58	2.51	2.56	1.72	2.41	0.92	28.07	103.86	58.84	986.89	767.78	350.78	148.11	122.91	94.99	165.78	10.13	17.27	242.67	6,15489	24.22
SD	0.07	0.36	0.30	0.25	1.05	0.28	0.16	2.43	14.63	15.90	551.00	263.88	123.45	23.48	26.60	15.14	33.18	1.95	3.81	53.98	3,572.74	6.74
c_{CC}/c_{UCC}	1.05	1.12	1.14	0.61	0.44	0.71		2.55	1.73	1.68	49.34	30.71	2.41	1.22	4.10	1.48	6.38	11.51	7.85	6.60	11.19	2.26
UCC																						
Aver.	0.50	4.99	2.20	4.20	3.90	3.40		11.00	60.00	35.00	20.00	25.00	145.60	121.70	30.00	64.00	26.00	0.88	2.20	36.75	550.00	10.70
NASC																						
Aver.	0.70	5.67	2.86	3.63	1.14	3.97	0.13	15.00	130.00	125.00	58.00		142.00	200.00	31.00	67.00	27.40	1.20	3.10	35.00	636.00	12.30
MORB Pacific Ocean																						
Aver.	1.66	11.40	7.62	11.67	2.78	0.16	0.17	39.12	319.60	254.40	95.67	85.85	145.60	121.70	4.97	13.74	10.35	1.29	3.07	36.75	31.40	0.57
SD	0.39	1.36	0.83	0.73	0.30	0.15	0.07	4.39	47.02	117.70	44.52	39.48	62.98	47.29	5.32	9.50	4.91	0.34	0.77	5.88	43.87	0.90
c_{MORB-P}/c_{UCC}	3.31	2.28	3.47	2.78	0.71	0.05		3.56	5.33	7.27	4.78	3.43	1.00	1.00	0.17	0.21	0.40	1.46	1.40	1.00	0.06	0.05
MORB Indian Ocean																						
Aver.	1.27	9.41	8.22	10.91	3.26	0.15	0.27	31.80	–	714.30	154.70	86.00	144.50	125.00	3.88	11.86	9.54	1.10	2.75	31.90	14.08	0.35
SD	0.19	0.82	0.58	0.69	0.56	0.08	0.03	0.53		210.70	50.24	13.08	46.04	56.00	1.43	4.17	2.10	0.15	0.33	7.00	7.01	–
c_{MORB-I}/c_{UCC}	2.53	1.89	3.73	2.60	0.84	0.04		2.89		20.41	7.74	3.44	0.99	1.03	0.13	0.19	0.37	1.25	1.25	0.87	0.03	0.03

Also shown are values for the North American Shale Composite (NASC; extracted from Gromet et al. 1984), the Pacific and Indian Ocean MORBs (extracted from Klein and Langmuir 2001), and the upper continental crust (UCC; extracted from Taylor and McLennan 1985). Major elements (as oxides) are expressed in percents, trace elements in mg/kg (ppm)

Geo-Marine Letters, 2009, 29(2), 71-83, doi : 10.1007/s00367-008-0123-5.

Table 2: Correlation analyses (matrixes of coefficients of correlation) for the contents of major components and trace elements with and without Ni and Cu in the Clarion-Clipperton nodule, micronodules and abyssal clay, as well as the upper continental crust (UCC) and the Pacific and Indian Ocean MORBs

	Nodule (nucleus)	*Nodule (envelope)*	*Micronodules*	*Abyssal clay*	*UCC*	*MORB Pacific*
6 major components: TiO_2, Fe_2O_3, MgO, CaO, Na_2O, K_2O, P_2O_5						
Nodule (envelope)	*0.9710*					
Micronodules	0.7307	0.5620				
Abyssal clay	*0.9156*	*0.9804*	0.4337			
UCC	0.7904	0.7480	0.6300	0.7657		
MORB Pacific	*0.9018*	0.8101	*0.8187*	0.6794	0.5411	
MORB Indian	*0.8505*	0.7462	*0.8127*	0.6043	0.5035	*0.9855*
15 trace elements: Sc, V, Cr, Ni, Cu, Sr, Y, Zr, Ba, La, Ce, Nd, Eu, Yb, Th						
Nodule (envelope)	*0.9633*					
Micronodules	*0.9985*	*0.9698*				
Abyssal clay	0.2776	0.5212	0.3019			
UCC	0.0526	0.3060	0.0769	*0.9397*		
MORB Pacific	0.0434	0.0083	0.0278	−0.1106	0.0007	
MORB Indian	0.0461	0.0120	0.0343	−0.1139	−0.0744	*0.6684*
13 trace elements: Sc, V, Cr, Sr, Y, Zr, Ba, La, Ce, Nd, Eu, Yb, Th						
Nodule (envelope)	*0.9970*					
Micronodules	*0.9853*	*0.9798*				
Abyssal clay	*0.9926*	*0.9990*	*0.9741*			
UCC	*0.9809*	*0.9724*	*0.9546*	*0.9651*		
MORB Pacific	−0.0633	−0.0945	−0.1196	−0.1153	0.0096	
MORB Indian	−0.1249	−0.1230	−0.1630	−0.1204	−0.0662	*0.6679*

Values in italics denote significant correlations at $p<0.05$ (95% probability)

Geo-Marine Letters, 2009, 29(2), 71-83, doi : 10.1007/s00367-008-0123-5.

Tables 3: Matrixes of correlation coefficients for both major and trace elements of the Clarion-Clipperton nodule, micronodules and abyssal clay

	TiO_2	Fe_2O_3	MgO	CaO	Na_2O	K_2O	P_2O_5	Sc	V	Cr	Ni	Cu	Sr	Y	Zr	Ba	La	Ce	Nd	Eu	Tb
Nodule																					
Fe_2O_3	0.9399																				
MgO	0.2473	0.0073																			
CaO	−0.6867	−0.7961	0.3771																		
Na_2O	−0.8105	−0.7358	−0.1158	0.6334																	
K_2O	0.8211	0.8214	−0.0543	−0.7556	−0.7824																
P_2O_5	−0.5603	−0.7171	0.4668	0.9613	0.4909	−0.5580															
Sc	0.7726	0.6737	0.1930	−0.4852	−0.8641	0.8714	−0.2626														
V	−0.7257	−0.7302	0.1597	0.7177	0.8229	−0.9716	0.5186	−0.8857													
Cr	0.4475	0.4045	−0.2923	−0.4652	−0.4233	0.7746	−0.2605	0.6551	−0.7936												
Ni	−0.7707	−0.7908	0.1827	0.7715	0.8229	−0.9814	0.5877	−0.8695	0.9942	−0.7805											
Cu	−0.7994	−0.8249	0.1368	0.8060	0.8584	−0.9763	0.6336	−0.8702	0.9821	−0.6994	0.9914										
Sr	−0.6742	−0.7214	0.2452	0.8286	0.7723	−0.9463	0.6624	−0.7800	0.9658	−0.7281	0.9676	0.9720									
Y	−0.3261	−0.5343	0.5084	0.8146	0.1540	−0.3110	0.9193	0.0917	0.2395	−0.0718	0.3178	0.3605	0.4282								
Zr	0.6875	0.7334	0.1281	−0.489	−0.427	0.2352	−0.578	0.1886	−0.127	−0.199	−0.219	−0.270	−0.128	−0.497							
Ba	0.8609	0.7989	0.1081	−0.6459	−0.9404	0.8819	−0.4691	0.9631	−0.8888	0.5753	−0.8941	−0.9140	−0.8170	−0.1160	0.3973						
La	−0.3003	−0.5267	0.6030	0.8167	0.1623	−0.4623	0.8601	−0.0134	0.4138	−0.3007	0.4733	0.4877	0.5817	0.9361	−0.2760	−0.1590					
Ce	−0.4325	−0.4233	0.2054	0.5419	0.6404	−0.8488	0.3222	−0.7854	0.9187	−0.8231	0.8796	0.8508	0.9044	0.0756	0.2636	−0.7154	0.3155				
Nd	−0.4111	−0.6166	0.5652	0.8850	0.2889	−0.5716	0.9009	−0.1462	0.5248	−0.3770	0.5826	0.5994	0.6799	0.9246	−0.3172	−0.2928	0.9900	0.4083			
Eu	−0.5056	−0.6821	0.4863	0.9429	0.3946	−0.5943	0.9609	−0.2086	0.5414	−0.3342	0.6040	0.6368	0.6992	0.9431	−0.4325	−0.3821	0.9558	0.3889	0.9815		
Tb	−0.4455	−0.6483	0.5054	0.9088	0.3237	−0.5094	0.9577	−0.1169	0.4531	−0.2319	0.5209	0.5606	0.6243	0.9714	−0.4610	−0.3044	0.9619	0.2951	0.9753	0.9921	
Th	0.1437	−0.0049	0.4934	0.3518	−0.1927	0.0458	0.4621	0.2781	−0.0514	−0.0443	−0.0153	−0.0136	0.1022	0.5888	0.0006	0.2082	0.5870	0.0039	0.5324	0.4927	0.5183

Geo-Marine Letters, 2009, 29(2), 71-83, doi : 10.1007/s00367-008-0123-5.

	TiO_2	Fe_2O_3	MgO	CaO	Na_2O	K_2O	P_2O_5	Sc	V	Cr	Ni	Cu	Sr	Y	Zr	Ba	La	Ce	Nd	Eu	Tb
Micronodules																					
Fe_2O_3	0.5299																				
MgO	0.5338	0.2219																			
CaO	−0.6504	-0.5882	*−0.7623*																		
Na_2O	0.1201	0.5692	−0.0564	−0.3574																	
K_2O	0.5730	*0.7141*	−0.0230	−0.5619	0.4950																
P_2O_5	−0.0902	−0.0442	−0.6125	0.1070	0.5143	0.5044															
Sc	0.1611	0.0594	−0.457	−0.062	0.5125	0.6372	*0.9619*														
V	0.2305	−0.1525	*0.7581*	−0.2133	−0.3967	−0.5875	*−0.8547*	*−0.7809*													
Cr	0.4806	*0.7191*	−0.2725	−0.1194	0.4164	0.6618	0.2655	0.3764	−0.4013												
Ni	0.0791	−0.0980	*0.7768*	−0.2602	−0.2939	−0.5977	*−0.8680*	*−0.8401*	*0.9593*	−0.5056											
Cu	0.1562	0.1534	*0.7837*	−0.3540	−0.1347	−0.4417	*−0.8744*	*−0.8410*	*0.8936*	−0.3374	0.9635										
Sr	−0.4213	−0.6645	−0.4574	*0.9013*	−0.5505	*−0.7318*	−0.1816	−0.2776	0.1806	−0.1967	0.0628	−0.0743									
Y	0.0454	0.0961	−0.6092	0.0758	0.5425	0.6016	*0.9757*	*0.9571*	*−0.8592*	0.3967	−0.8886	−0.8547	−0.2043								
Zr	0.2957	−0.5282	0.1611	0.1377	−0.4077	−0.2937	−0.0541	0.0843	0.3750	−0.0832	0.1404	−0.0571	0.4468	−0.1098							
Ba	*0.7316*	−0.0724	0.2050	−0.2833	−0.0318	0.3747	0.3148	0.5266	0.0130	0.2186	−0.2060	−0.2898	−0.0866	0.3537	*0.7094*						
La	−0.0153	−0.0709	−0.5601	0.0940	0.5190	0.4802	*0.9903*	0.9738	*−0.7872*	0.2652	−0.8258	−0.8443	−0.1493	*0.9696*	0.0516	0.4144					
Ce	0.5162	−0.2211	0.1846	0.0226	0.0320	−0.1330	0.0708	0.2057	0.3494	0.0914	0.1398	0.0496	0.3099	0.1129	*0.7610*	*0.7519*	0.2056				
Nd	0.0358	0.0241	−0.6052	0.1053	0.5250	0.5433	*0.9816*	*0.9645*	*−0.8225*	0.3607	−0.8659	−0.8535	−0.1517	*0.9950*	−0.0271	0.3951	*0.9855*	0.1854			
Eu	0.0064	0.0518	−0.6214	0.1009	0.5408	0.5648	*0.9868*	*0.9632*	*−0.8566*	0.3721	−0.8863	−0.8649	−0.1785	*0.9976*	−0.0775	0.3490	*0.9823*	0.1213	*0.9976*		
Tb	0.0668	0.1523	−0.624	0.0693	0.5594	0.6362	*0.9667*	*0.9579*	*−0.873*	0.4759	−0.912	−0.868	−0.217	*0.9950*	−0.103	0.3482	*0.9586*	0.0981	*0.9872*	*0.9926*	
Th	0.1472	0.6096	−0.4550	−0.0887	*0.8106*	0.6510	0.6575	0.6339	−0.6812	0.6916	−0.6460	−0.4620	−0.3605	*0.7598*	−0.4800	0.0034	0.6358	−0.0325	*0.7211*	*0.7374*	*0.7859*

Geo-Marine Letters, 2009, 29(2), 71-83, doi : 10.1007/s00367-008-0123-5.

	TiO_2	Fe_2O_3	MgO	CaO	Na_2O	K_2O	P_2O_5	Sc	V	Cr	Ni	Cu	Sr	Y	Zr	Ba	La	Ce	Nd	Eu	Tb
Abyssal clay																					
Fe_2O_3	0.5401																				
MgO	−0.5421	0.1975																			
CaO	0.0527	0.2930	0.3127																		
Na_2O	*−0.8272*	−0.0429	0.5603	−0.0231																	
K_2O	*0.9412*	0.6202	−0.2557	0.1103	*−0.7902*																
P_2O_5	0.0593	0.4082	0.5214	*0.9297*	−0.0067	0.2256															
Sc	0.0590	0.5349	*0.7823*	0.4599	0.0336	0.3594	*0.7186*														
V	*0.7353*	0.0204	−0.5253	0.0547	*−0.8888*	*0.7208*	0.0838	−0.0364													
Cr	*0.7561*	0.0249	−0.8528	−0.2815	*−0.7563*	0.5974	−0.3373	−0.4633	*0.8358*												
Ni	−0.0383	−0.4623	−0.0393	0.4865	−0.3956	−0.0156	0.3795	−0.0301	0.4592	0.1128											
Cu	0.0068	−0.3437	−0.0628	0.6106	−0.3609	−0.0023	0.4568	−0.0416	0.4011	0.0893	*0.9746*										
Sr	−0.5623	0.1121	*0.9844*	0.3797	0.5143	−0.2846	0.5614	*0.7562*	−0.5161	*−0.8722*	0.0753	0.0525									
Y	0.4954	0.3591	0.1891	*0.7323*	−0.577	0.6458	*0.8091*	0.6450	0.5627	0.1057	0.5322	0.5614	0.2378								
Zr	−0.346	0.2329	*0.9104*	0.2134	0.3558	−0.022	0.5152	*0.8595*	−0.254	−0.628	−0.085	−0.168	*0.8796*	0.2943							
Ba	*−0.7276*	0.0553	0.9566	0.2294	*0.7470*	−0.4960	0.3904	0.6046	*−0.7170*	*−0.9407*	−0.1328	−0.1514	*0.9481*	−0.0453	*0.8262*						
La	0.0694	0.3184	0.6474	*0.7350*	−0.1485	0.3298	*0.8982*	*0.8670*	0.1825	−0.3453	0.4438	0.4475	*0.6844*	*0.8654*	*0.6882*	0.4517					
Ce	*0.8439*	0.3058	−0.4997	0.4041	*−0.8517*	*0.7804*	0.3247	0.0169	*0.8364*	*0.7005*	0.4699	0.5293	−0.4626	*0.7097*	−0.3823	*−0.6962*	0.2894				
Nd	0.2307	0.2759	0.4630	*0.7422*	−0.3575	0.4508	*0.8626*	*0.7773*	0.3541	−0.1724	0.5457	0.5544	0.5150	*0.9496*	0.5182	0.2455	*0.9705*	*0.4728*			
Eu	0.4724	0.3853	0.2102	*0.7735*	−0.5213	0.6203	*0.8485*	0.6571	0.5217	0.0711	0.5059	0.5454	0.2585	*0.9965*	0.3098	−0.0133	*0.8744*	*0.6880*	*0.9487*		
Tb	0.5630	0.2985	0.0548	*0.6972*	*−0.6688*	*0.6743*	*0.7405*	0.5410	0.6406	0.2118	0.5666	0.5918	0.1154	*0.9867*	0.1782	−0.1714	*0.7883*	*0.7815*	*0.9004*	*0.9784*	
Th	−0.4452	0.1245	0.0813	0.1430	*0.7632*	−0.5571	0.0402	−0.2330	−0.5669	−0.3066	−0.3678	−0.2490	0.0159	−0.4572	−0.0949	0.2563	−0.3024	−0.4294	−0.4202	−0.3939	−0.5180

All correlations significant at p< 0.05 are shown in italics